

JYU | Department of Particulate Flow Modelling

Annual Report | 2023

JKU DEPARTMENT OF PARTICULATE FLOW MODELLING

T +43 (0)732/2468 6477 | F +43 (0)732/2468 6462 | W <http://www.particulate-flow.at>
P | Altenbergerstrasse 69, 4040 Linz, Austria



Front cover: Science in a tuna can! In our annual seminar we looked into the interaction of an electric arc and a reservoir of tap water. The arc generated by an AC transformer induces a 100Hz wave pattern on the liquid surface. Interestingly, wave motion starts way before the arc is visible.
© S. Puttinger and the rest of the gang (see 15 Years of Curiosity)

EDITORIAL

Dear Readers,

“Bloody Fluid Dynamics” – this is how we entitled our 2012 seminar lecture. Each year, we all together embark on a specific topic we are not familiar with. Together with a bunch of interested students we approach a new field by (i) analytical considerations, (ii) numerical simulation and (ii) experiments (yes, we looked at our own blood cells).

Regularly, this curious look over the fence actually transforms into science. “Bloody Fluid Dynamics” resulted in up to now two PhD works, novel modelling approaches and a couple of scientific publications. One of our first seminars on “Slow Granular Flow” even triggered world-wide research activities.

This year’s seminar is called “Lightning Fluid Dynamics” and once again we embark on something new. After learning the basic ingredients of plasma physics, we aim to cook some novel simulation tools based on our multi-scale, data-assisted and physics based modelling skills. Maybe, we could thus contribute to process electrification in the realm of industrial decarbonization.

With these introducing words, I wish you a pleasant reading!

All the best.



EDITORIAL

Dear Readers,

“Talk is cheap. Show me the code.” (Linus Torvalds). There is hardly any other phrase that would be more appropriate to describe our day-to-day research activities over the past year – though some might arguably replace “code” by “equations”.

Since the very beginning, software development at PFM had a strong focus on open source which – unlike proprietary software – empowers us to collaborate and share knowledge with great freedom.

The most prominent examples are **LIGGGHTS** and **CFDEMcoupling** which are well-recognized and used by researchers across the globe. While we are still maintaining and expanding those tools, we did not stop there and for example also regularly make our purely OpenFOAM-based models available via the **pfmFOAM** project.

Last but not least, the introduction of the **rCFD** method unleashed a whole new level of software development where we are aiming to provide a reference implementation of the underlying algorithms. While designing this software is an exciting task, it is also a challenge and definitely a matter of passion to create a sound and comprehensive tool.

Even though these activities are typically outshined by simulation results, they are nevertheless an essential backbone of our group's research. If we sparked your interest in this side of our work, follow us at **github.com/ParticulateFlow**. In case our tools help you complete your project or trigger new ideas for collaborations we would be more than happy to hear about it.



Sincerely,

Daniel Quetschiner

CONTENTS

MICRO

Unresolved CFD-DEM Simulation of Red Blood Cells	6
Detachment of a Soluble Particle at the Slag-Argon Interface.....	8
Resolved Simulation of Bubbly Flow in Metallurgical Application.....	10
How do the Droplets and Bubbles Fragment in Turbulent Flows?.....	12
Compressible VOF Simulation of Submerged High-Speed Gas Injection into Liquid	14

MESO

Particle Coating Using a Discrete Droplet Method	18
Modeling of Fine Cohesive Powders	20
The Multiphysics and Multi-Scale Challenge of Blast Furnace Simulations	22

MACRO

A Hybrid Continuum-Discrete Method for Simulating Particle-Laden Flows.....	26
On the Road to Green Steel Production	28
Fast Simulation of a Tundish Using Recurrence CFD	30
Deflagration	32

EXPERIMENTS & DATA ANALYSIS

Dust Deflagration	36
Data Compression with Autoencoders	38
rCFD - Virtual Shadow Demonstrator	40
Blast Furnace Tapping Behavior	42
Marangoni Driven Micro-Droplet Generation	44
Self-Sustained Marangoni Flows.....	46

SEMINAR 15 Years of Curiosity	48
--	----

SCIENTIFIC FRIENDS	50
---------------------------------	----

SELECTED PUBLICATIONS	52
------------------------------------	----

EDITORIAL | MICRO

Dear Readers,

Resolved small-scale simulations, when performed properly, disclose amazing facts about the physics of complex fluid flows. In multiphase flows, the role of such studies is even more crucial due to the well-known limitations of experimental characterization, and they serve as *numerical experiments* for many applications. In the past year, our research strategy has focused on such studies in different multiphase flows.

Carmine Porcaro continued his resolved immersed boundary-based simulation to find new correlations for the unresolved cell-level blood flow simulation, incorporating the physics of deformable RBCs. **Xiaomeng Zhang** managed to obtain a small-scale picture of the Marangoni effect on the particle dynamics at the steel-slag interface, which helps to develop models for non-metallic inclusion removal in large-scale simulation. Our new member, **Mohammad Karimi Zand** has just started his PhD in modelling and simulation of bubbly flows, aiming to address shortcomings in unresolved large-scale simulations of bubble plumes in the metallurgical application. We also started an in-house collaboration with the Institute of Process Engineering at JKU based on a FWF-funded project on bubble-particle interactions. **Enatri Enan** has joined us to focus on small-scale three-phase simulations using the immersed boundary and volume of fluid method. Our research on the theory of multiphase turbulence as well as compressible interfacial flows has also advanced in the past year, and we aim for more theoretical contributions to these fields in the upcoming year.



I hope you enjoy reading about our recent scientific journey!





Fig.1: Resolved simulation of red blood cells in different microfluidic conditions using the immersed-boundary method coupled with a reduced-order RBC model.

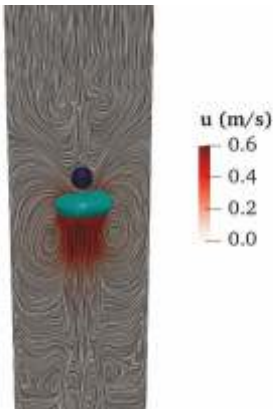


Fig.2: Resolved simulation of a freely-rising air bubble in water interacting with a falling rigid particle, using a coupled VOF-IB method.



Fig.3: Interface-resolved simulation of supersonic air injection into liquid in the near-nozzle region using the compressible VOF method and large eddy simulation.

MICRO | UNRESOLVED CFD-DEM SIMULATION OF RED BLOOD CELLS

Numerical simulation of blood flow is a challenging topic due to the multi-phase nature of this biological fluid. The choice of a specific approach among the ones available in literature is often motivated by the physical scale of interest. Single phase approximation allows for lower computational time, but does not consider this multi-phase nature. Nevertheless, red blood cells (RBCs) dynamics is responsible for many macroscale phenomena such as Fahraeus–Lindqvist effect, which leads to an increase in blood relative apparent viscosity and discharge hematocrit. RBCs are subjected to deformation, cross-stream migration, hemolysis, and aggregation, which need to be correctly taken into account for physically sound numerical simulation of blood.

This year, we focused on a scale-up strategy to allow the numerical simulation of blood flow in large scale domain using unresolved CFD-DEM simulations. We obtained data from our previously developed RBCs reduced-order model, and used it to build models for unresolved simulations (see Figure 1). Figure 2 shows the formation of a cell-free layer (CFL) in a large channel. This is the main cause of the increase in the discharge hematocrit and apparent relative viscosity, which both depend on the initial channel hematocrit and diameter. CFL has important applications also in the biomedical field, since it is the foundation of several microfluidics blood plasma separation techniques.

Future perspectives include improvement of the model with specific attention to particle-particle interactions, as well as coupling between resolved and unresolved approaches.

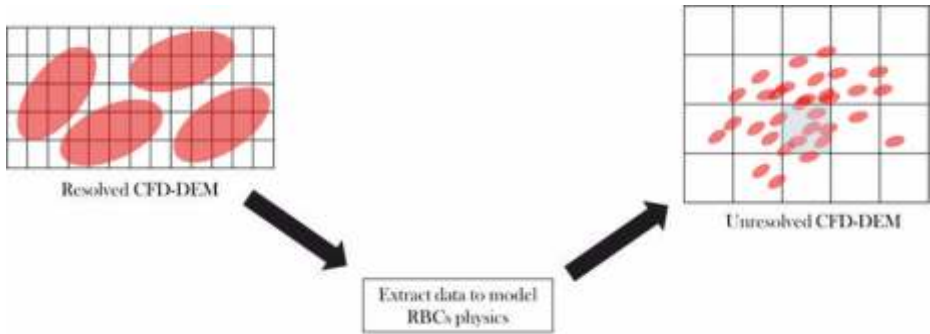


Fig.1: Schematics of the modelling strategy for unresolved RBCs.

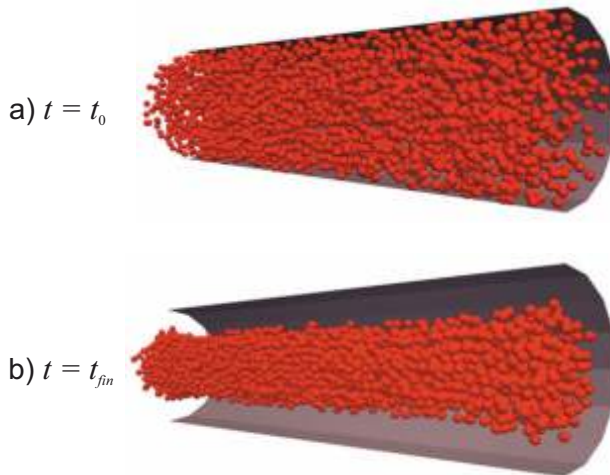


Fig.2: Unresolved simulation of blood flow in a large channel: a) initial timestep of the simulation t_0 b) final timestep of the simulation t_{fin} . Fluid-particle interactions are modelled: this helps to reproduce important macroscale phenomena such as CFL formation.



MICRO | DETACHMENT OF A SOLUBLE PARTICLE AT THE SLAG-ARGON INTERFACE

Studying the behavior of a micron-sized particle at the steel-slag interface has been a central topic of this work, which is essential for understanding the inclusion removal mechanism. By means of high-temperature confocal laser scanning microscopy (HT-CLSM), it is possible to access such an environment of steelmaking temperatures and observe particle behavior in it in situ. One of the most representative experiments is the dissolution of an oxide particle in molten slag. The experimental setup is schematically shown in Fig. 1. The interest in particle dynamics near the interface draws our attention to the stage of particle moving across the slag-argon interface. A set of frames from the corresponding experiment is presented in Fig. 2. After the slag melts, it is observed that the particle initially located on the slag surface falls into the slag rapidly and settles at the interface with a small area exposed to argon. In addition, experiments reveal that after a relatively long time, the particle finally detaches from the interface with a significant morphology change. The dynamic motion of the particle, which is driven by capillary force, can be well depicted by CFD simulations using the VOF method and the dynamic overset mesh. Further considering particle dissolution, investigations indicate that the concentration variation near the interface arising from dissolution enables to trigger a Marangoni flow. This flow, in turn, enhances the local dissolution rate (as indicated by Fig. 4, more mass flux along particle surface in the case with the Marangoni effect involved), which could be responsible for the significant particle shape change and lead to the final particle detachment.

The study indicates that both particle dynamics and particle dissolution govern the particle detachment from the slag surface, which can be relevant to inclusion removal through slag absorption in metallurgical processes. This work has been documented as a journal paper wherein more details are available.

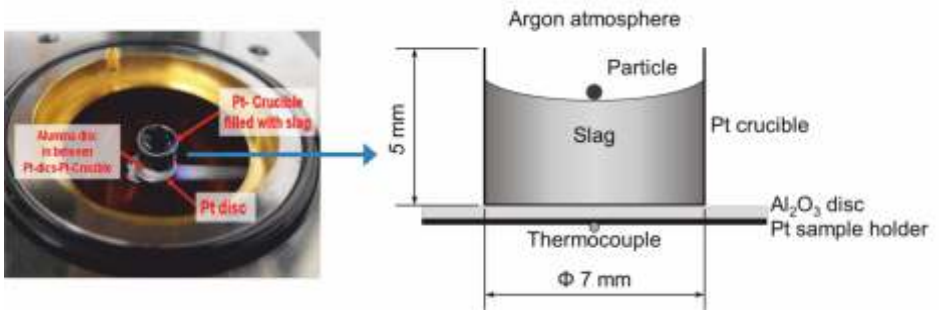


Fig.1: Sample placed in the high-temperature chamber of HT-CLSM; setup for dissolution experiment.

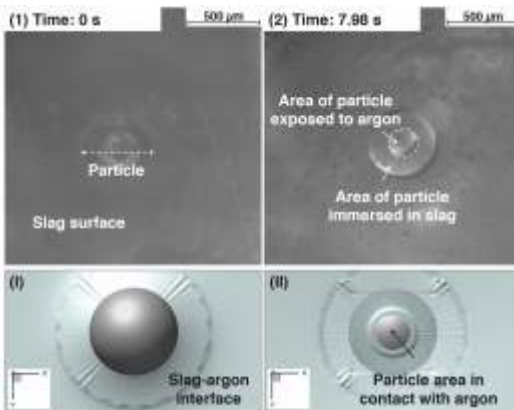


Fig.2: Particle moving across the slag-argon interface by experimental observation (upper row) and simulation (lower row).

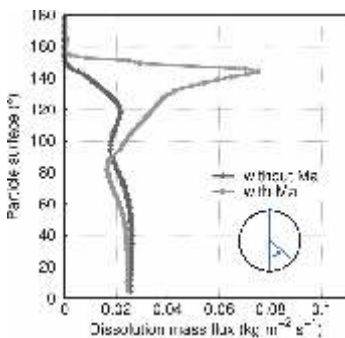


Fig.3: Dissolution mass flux along particle surface in the situation with and without the Marangoni effect involved.



MICRO | RESOLVED SIMULATION OF BUBBLY FLOW IN METALLURGICAL APPLICATION

Bubbly flow, which is characterized by distinct bubbles in a liquid flow, is an important flow regime in many industrial processes. In many metallurgical applications, gas injection and steering caused by the bubble plume is an integral part of the process. Examples are the removal of hydrogen in the degassing of aluminum or the removal of non-metallic inclusions from steel in the ladle or tundish. Thus, accurate prediction of these bubble flows is of great importance. In many metallurgical processes, CFD has become a useful tool to analyze and optimize, but a fundamental understanding of the effect of injection method and nozzle size, bubble properties, shapes, rising velocities, or interfacial forces is crucial for the understanding, modeling, and optimization of bubble column reactors.

Henceforth, we are focused on investigating the characteristics of bubble plumes in liquid steel. At first, we are interested in the effect of different operating parameters like nozzle size, nozzle wettability, and gas flow rate on bubble generation. In addition, since it is well known that liquid properties also have drastic effects on bubble size and shape, the influence of density, viscosity, and surface tension will also be studied. To have a deeper understanding of the behavior of the bubbles rising inside the plume, sufficient knowledge of the forces acting on the bubbles in different conditions is required.

We have started by performing single bubble simulations in an air-water system using OpenFOAM (the geometric VOF solver of interIsoFoam). To validate the results and gain confidence in the simulations and methodology, we are planning to conduct lab experiments with the time-resolved PIV technique. These resolved numerical simulations together with the experimental measurements will provide enough knowledge to develop force models for the bubble dynamics in large-scale bubble plume simulations using Eulerian-Lagrangian coupling, which is planned for the next steps of the project.

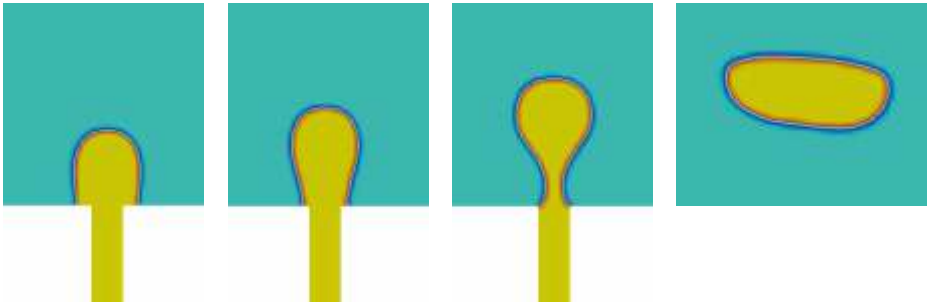


Fig.1: Different stages of single air bubble generation from a 2-mm orifice in water.

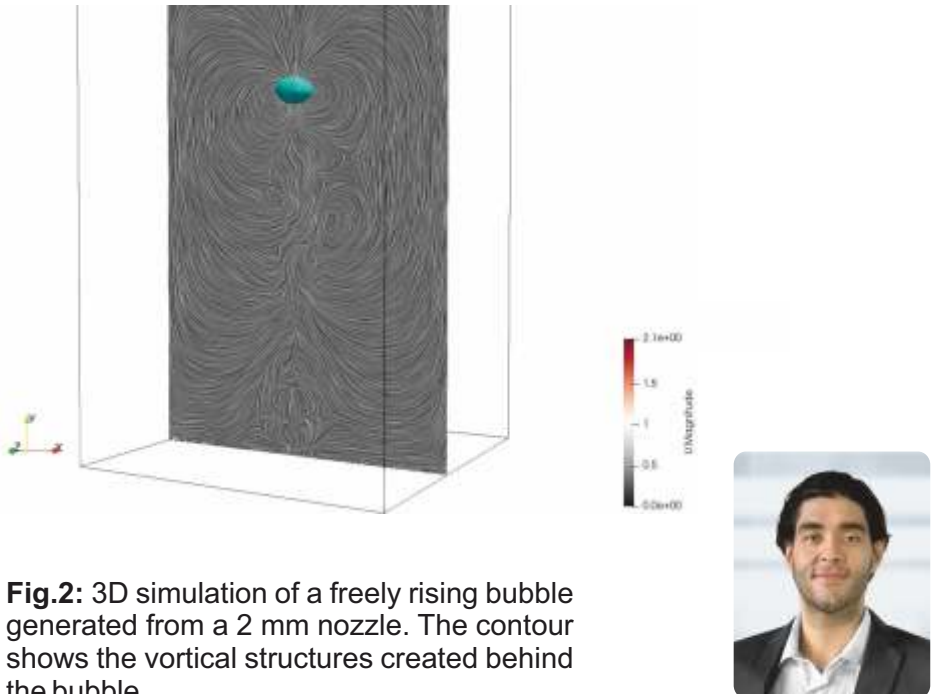


Fig.2: 3D simulation of a freely rising bubble generated from a 2 mm nozzle. The contour shows the vortical structures created behind the bubble.

MICRO | HOW DO THE DROPLETS AND BUBBLES FRAGMENT IN TURBULENT FLOWS?

Scale-dependent nature of the turbulence modulations in droplet-laden or bubbly flows mandates the determination of characteristic length scales to provide adequate grid resolutions in highly-resolved two-phase flow simulations. One such length scale is the size of the largest stable droplets or bubbles that could appear as the result of fragmentation in turbulence. This length scale is called the Kolmogorov-Hinze (K-H) scale (named after the seminal works of Andrey N. Kolmogorov (1949) and Julius O. Hinze (1955)), and has been the subject of several important research in the past decades. Nevertheless, the original correlation of the Kolmogorov-Hinze scale was developed for specific cases and contains constant values that are proportional to the droplet critical Weber number, which may limit its general applicability for different conditions.

Based on the fully-resolved VOF simulations of fragmentation of a thin sheet in homogeneous isotropic turbulence (HIT) (Figure 1), we analyzed the spectral contribution of different vorticity transport mechanisms and observed a critical length-scale ($2\rho/\kappa_c$) where the enstrophy cascade of a droplet-laden HIT deviates from the single-phase one. Our analysis unveils that this critical length scale corresponds to the size of eddies for which the vortex stretching is unable to drive the cascade further, and the eddy breakup events are not the source of energy transfer. In other words, the spectral rate of enstrophy transfer by surface tension can resist vortex stretching rate at κ_c as shown in Figure 2. We further demonstrate that the size distribution of droplets also changes the slope at this critical length scale as shown in Figure 3.

The correlation between turbulence statistics, specifically enstrophy rates, and the fragmentation statistics, represented by size distribution, elucidates the process of droplet and bubble fragmentation within turbulent flows. Moreover, the new interpretation of the K-H scale based on the concept of enstrophy could serve as a valuable tool to determine the size of dispersed droplets and bubbles as a consequence of the variation in the turbulent flow quantities. These findings are still subject to further investigation in non-decaying forced HIT conditions.

Fig.1: Instantaneous snapshot of the droplets generated out of the turbulent fragmentation process. The Weber number associated with the initial sheet thickness is 110, and no density and viscosity contrast is assumed. The structures are visualized by the iso-surfaces of 50% volume fraction [1].

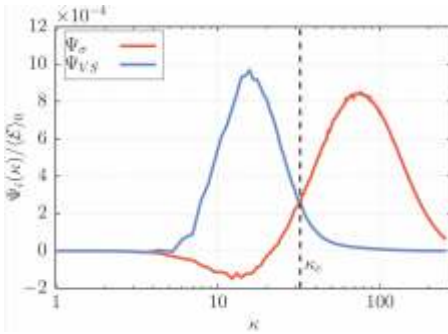
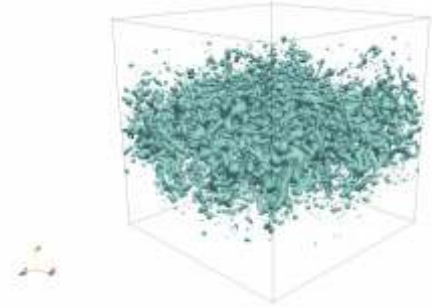


Fig.2: Normalized spectral rates of vortex stretching (Ψ_{VS}) and surface tension (Ψ_c) terms to the enstrophy generation across the scales at the same instant of fragmentation shown in Figure 1. The dashed vertical line shows the intersection wave number κ_c .

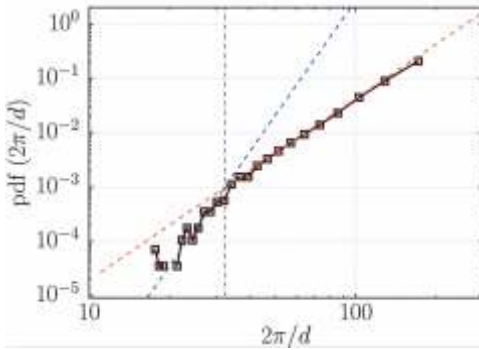


Fig.3: Size distribution of droplets at the same instant of time as a function of corresponding wave-number. The blue and red dashed lines are fitted to track the change in the PDF slope, and the dashed vertical line shows the same κ_c as in Figure 2 [1].



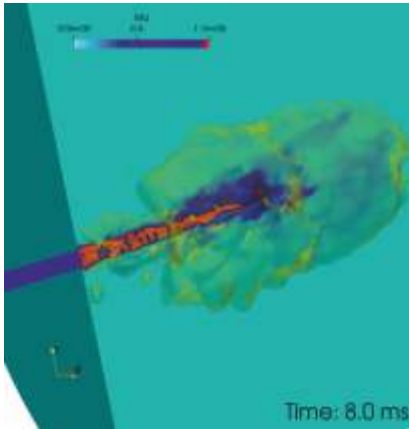
[1] Saeedipour M., An enstrophy-based analysis of the turbulence-interface interactions across the scales, International Journal of Multiphase Flow 164, 104449, 2023.

MICRO | COMPRESSIBLE VOF SIMULATION OF SUBMERGED HIGH-SPEED GAS INJECTION INTO LIQUID

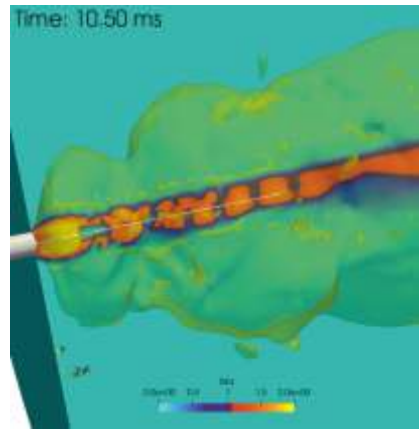
Massive, submerged, high-speed gas injection into liquid constitutes a complex multiphase flow with various applications in metallurgical plants such as argon-oxygen decarburization (AOD) converter. An in-depth understanding of the flow physics in such extreme conditions is still lacking in the literature. While conducting experimental measurement is always cumbersome, the numerical simulation is not straightforward too, due to several sources of complexity such as turbulence, gas compressibility, shock formation, and shock-interface interactions. In the context of finite-volume CFD methods, the presence of supersonic jets and shock formation demand high spatial and temporal resolutions and low Courant numbers. Also, the gas compressibility urges additional numerical treatments to overcome numerical instability. Moreover, the fragmentation of interfacial structures and small-scale bubble formation impose more computational costs due to the typical time-step constraint to capture the surface tension force properly. These limits the applicability of interface-resolved techniques such as the VOF method to large-scale simulations.

Using the compressible VOF method, we have performed a small-scale interface-resolved LES simulation of air-to-water injection at the near-nozzle region. In these 3D simulations, the gas injection is initiated by a pressure gradient at the inlet of the nozzle to establish a two-phase gas-liquid flow with compressibility effects. Depending on the injection pressure, the flow could become supersonic and the simulation results clearly demonstrate the shock formations downstream of the nozzle. By increasing the injection pressure, the flow experiences higher Mach numbers and the shocks become stronger as evident from the pressure distribution downstream the nozzle shown in Figure 1. These simulations are validated against macroscopic quantities from experiments showing reasonable agreements e.g. for the mass flow rate and Mach numbers. Considering the acknowledged limitation of the optical measurement techniques in this context, these simulations offer a basis for the physical interpretation of shock-related processes such as the Richtmyer-Meshkov instability and the back-attack phenomenon. The latter is thought to be attributed to the traveling shocks, their reflection and interference, as well as their interaction with the liquid-gas interface.

Future studies are planned to explore the back-attack phenomenon based on these highly-resolved simulations.



$P_{inlet} = 2.8 \text{ bar}$



$P_{inlet} = 7.5 \text{ bar}$

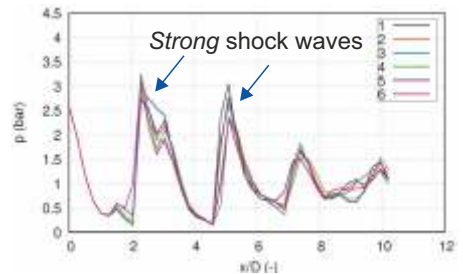
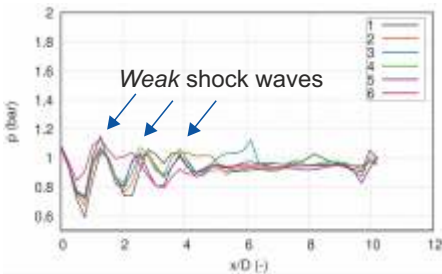


Fig.1: Instantaneous snapshots of the 3D compressible VOF simulation of massive gas injection into water at different inlet pressures of 2.8 and 7.5 bars, with the contour of Mach number (top row). The pressure distribution over a line downstream of the nozzle demonstrates traveling shocks and pressure waves inside the gas core (bottom). The pressure distribution is plotted at different times with 0.1 ms intervals to track the local changes attributed to traveling of the waves.



EDITORIAL | MESO

Dear Readers,

Many definitions can be found what "mesoscopic research" actually means. We regard it essential that it is not only located between something smaller ("microscopic") and something larger ("macroscopic"), but that it also establishes a connection between these two extremes and provides a way to transfer information across the scales.

For this reason, mesoscopic modeling and simulation activities span a broad range with regard to both topics and methods. Furthermore, knowledge increase often happens in a multidirectional fashion: Improving existing tools and/or applying them to new applications is equally important as developing novel techniques.

Over the last few years, Daniel Queteschiner has continuously advanced his embedded discrete-element simulations and is now tackling full-scale shaft furnaces displayed in Fig. 1. Marco Atzori, who has left our group to the Polytechnic University of Milan, used state-of-the-art particle-fluid simulations to devise a new, minimally invasive strategy to counteract segregation in fluidized bed reactors. Hannes Lumetzberger has recently joined us to bridge the gap between short and long time scales in turbulent flows by further developing our time-extrapolation techniques. Tobias Kronlachner created a completely novel workflow to characterize cohesive powders and obtain mesoscopic material parameters, which allows him to simulate such systems with astonishing accuracy. For example, he can picture die filling processes as shown in Fig. 2 in a reliable fashion.

I hope that you find these research directions as fascinating as I do, and that you cannot wait to read more about some of them on the next few pages.



Sincerely,

A handwritten signature in black ink that reads "Thomas Lichtenegger". The signature is written in a cursive style with a long, sweeping tail on the last letter.

Fig.1: Gas flow through a full-scale MIDREX shaft furnace. The velocity stream lines (left) and the transient temperature field during heating up (right) demonstrate that a fraction of the inflowing gas first moves downwards before it makes its way to the outlet at the top.

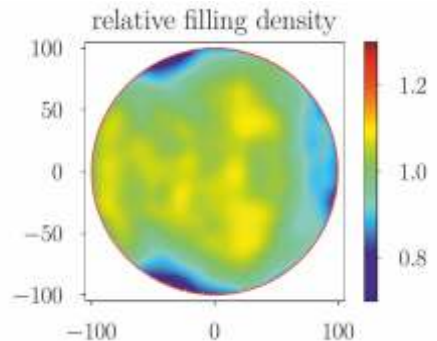
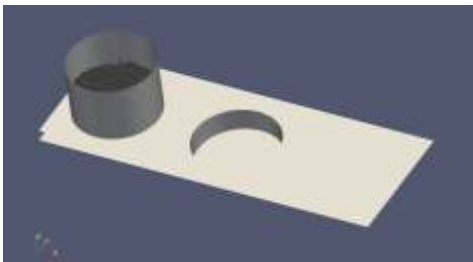
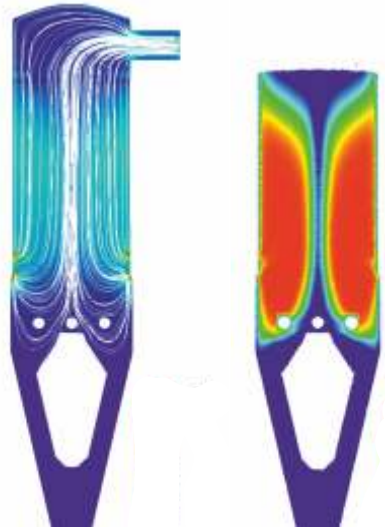


Fig.2: Die filling simulation with optimized DEM parameters. (left) A cylindrical filling shoe moves powder over a die. (right) The density profile of the filled die shows heterogeneities at some locations close to the wall. Only the use of optimized material parameters leads to realistic predictions.

MESO | PARTICLE COATING USING A DISCRETE DROPLET METHOD

Coating of granular materials is widely applied in industrial processes. In the pharmaceutical industry, for instance, tablets are usually spray-coated for functional or non-functional reasons. Functional coating layers are generally used for taste or odor masking, humidity protection, or modified release of the active pharmaceutical ingredient, whereas non-functional coatings are commonly used to improve the product's aesthetic appearance and recognition values. Especially in functional coatings, the drug release strongly depends on the film coating thickness.

Coating uniformity is important for both functional and non-functional coating. The two indicators of coating quality are inter-particle coating uniformity and intra-particle coating uniformity. The inter-particle coating uniformity reflects the overall uniformity among all particles. The intra-particle coating uniformity indicates the coating distribution on a single particle. Typically, inter-particle coating uniformity is related to the particle movement in the coating area and intra-particle coating uniformity is associated to the particle rotation in the coating area.

To obtain additional properties related to coating (e.g., coating uniformity) in a DEM simulation, it must be established which particles are in the spray region at a given time. Different approaches to this problem have been proposed such as top-detection or ray-tracing algorithms to monitor the residence time in the spray zone or including spray droplets directly into the DEM simulation.

In this preliminary study we opted for the latter approach and implemented the Discrete Droplet Method (DDM) to simulate spray coating. All spray droplets are assumed to be spherical, and the contacts between droplets are ignored. After the contact between a droplet and a particle, the droplet mass is added to the particle and the droplet is removed from the system. Since the coating layer is relatively thin, only the change of particle mass is considered here and the change of particle volume is neglected.

Spray residence time is connected to the particle velocity in the spray zone as well as the spray pattern. A narrow distribution of time in the spray zone is favorable as the amount of coating material that each particle receives is more uniform and the risk of over-wetting is reduced.

A wide distribution means that particles with higher residence times have an increased risk of over-wetting. This may cause defects such as particles sticking to each other or to the wall. Figure 1 illustrates three of the most basic spray patterns produced by different nozzles: (a) Full cone nozzles produce a solid circle of spray. (b) Hollow cone nozzles produce a ring of spray. (c) Flat fan nozzles produce a line of spray.

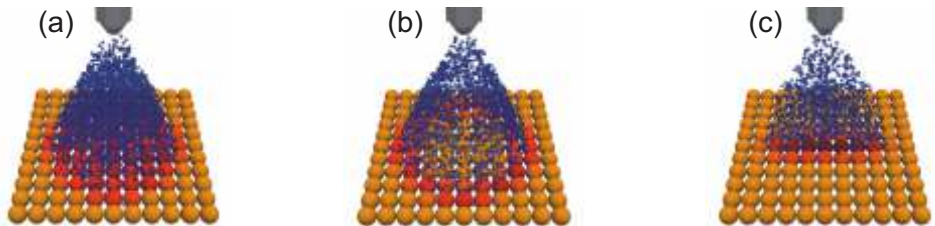


Fig.1: (a) full cone nozzle, (b) hollow cone nozzle, (c) flat fan nozzle.

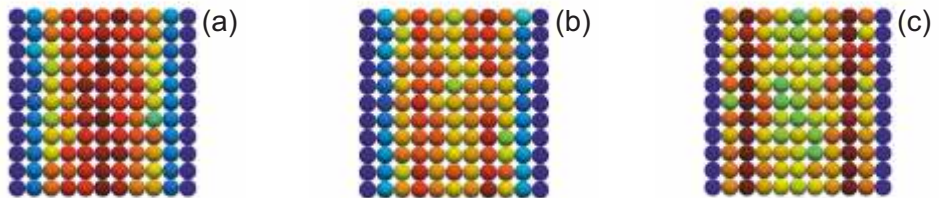


Fig.2: Inter-particle coating uniformity for (a) a full cone nozzle, (b) a hollow cone nozzle with small inner radius, (c) a hollow cone nozzle with large inner radius.

If the particles pass under the spray or – as in this case – the spray nozzle is moved forth and back over the particles, we can observe the influence of the spray patterns on the inter-particle coating uniformity. We notice that for a full cone nozzle, the particles close to the cone center receive more coating material since their spray residence time is longer compared to the outer cone section (Fig. 2a).

To some extent this issue can be alleviated by using a hollow cone nozzle instead (Fig. 2b). However, if the ring produced by the hollow cone nozzle is chosen too narrow, we run into a similar problem as for the full cone nozzle, this time causing more coating material deposited on the particles in the outer cone region (Fig. 2c).



MESO | MODELING OF FINE COHESIVE POWDERS

The processing of granular material is of importance in many fields. One example is powder metallurgy, which is essential for producing highly specialized components. The industrially used powders often consist of small, irregular particles with dominating cohesive forces. A reliable computer simulation is vital to understand how these powders behave in different flow situations. The discrete element method (DEM), a simulation tool that represents the material by distinct particles, can be utilized to model the flow behavior of such materials. However, it relies on material parameters, which can be challenging to estimate for these cohesive powders, especially in the low consolidation state regime.

For this reason, validation of the created model is vital. We investigated a cylindrical die filling process (Fig 1. and Fig. 3), where we built an experimental and a simulation model of the same geometry. To compare the results of both setups we developed a method to distinguish quantitative measurements from the experimental setup. The stencil to split the material in the die into quarters and the split bottom of the die is shown in Fig. 2.

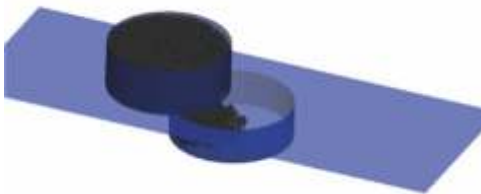


Fig.1: Filling process simulation model. Filling of a cylindrical die with a cylindrical filling shoe with one forward and one backward pass.



Fig.2: Stencil and die bottom. The stencil used to split the material and the bottom to empty the die quarters separate.

The mass of the quarters can be compared between the experimental setup and the simulation model. The results demonstrating the capabilities of the model describing this process are shown in Fig. 4. Ultimately, our research aims to use this model to improve the filling result by improving the filling shoe geometry as well as the moving speed of the shoe during the filling process.

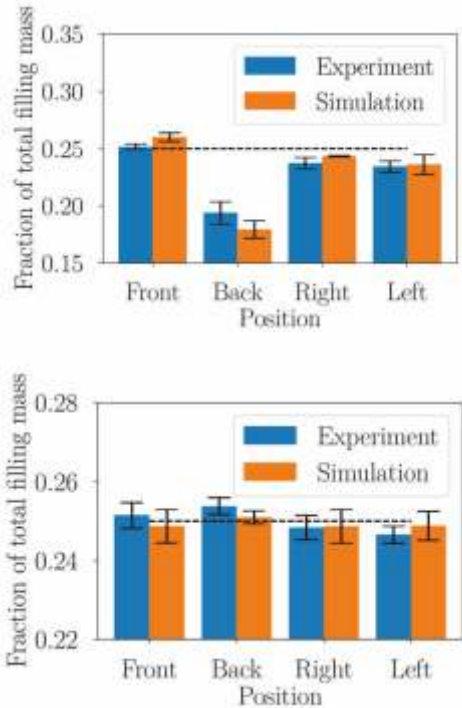


Fig.4: Filling process. Filling of a cylindrical die with a cylindrical filling shoe with one forward and one backward pass.

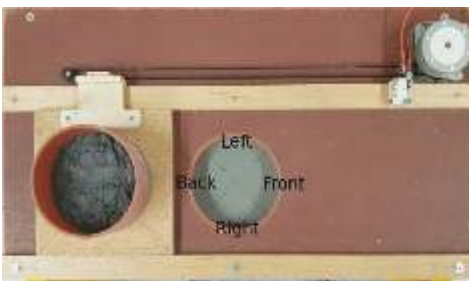


Fig.3: Filling process experimental setup. Filling of a cylindrical die with a cylindrical filling shoe with one forward and one backward pass.



MESO | THE MULTIPHYSICS AND MULTI-SCALE CHALLENGE OF BLAST FURNACE SIMULATIONS

Moving bed reactors in general and blast furnaces in particular are prime examples for multiscale problems. Particle-scale processes with short time-scales (grain contacts, local interfacial heat and mass transfer) determine the global properties of the reactor over long durations, i.e. the thermo-chemical steady state. In order to obtain this state, one needs to model the coupled mechanical, thermal and chemical processes in a way that (i) respects the underlying laws of physics and (ii) allows to decouple the short and small from the large and long scales.

Over the last few years, we have developed such a framework that combines high-fidelity DEM data with fast, long-term simulations. Hypothesizing that the granular and the gas motion change only slowly (“pseudosteady conditions”), we can carry out simulations over process-relevant durations of many hours until the thermo-chemical steady state is reached. Of course, models for the various physical and chemical phenomena are included in our calculations. As always with mesoscopic modeling activities that aim to bridge scales, their choice is a compromise between detailedness and numerical costs. For example, radiative heat transfer is captured in terms of an effective conductivity for a packed bed, and the complex multi-step reduction of hematite to magnetite, wustite and finally to iron is described with a multi-layer shrinking core model.

The results for the thermo-chemical steady state of a full-scale blast furnace can be seen in Figs. 1 and 2. After 20 hours of process time, the particle temperature field including the location of the cohesive zone has converged, and a chemical reduction state with mostly iron at the upper edge of the cohesive zone has established.

This type of simulation opens the door to explore process variations and their long-term impact, which may be useful for optimization purposes or the development of novel reactor types.

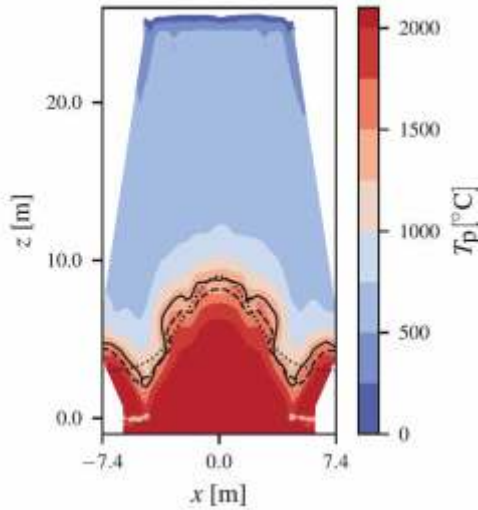


Fig.1: Converged particle temperature field after 20 hours process duration. The lines indicate the evolution of the cohesive zone after ten hours each. The upper part of the furnace, where the temperature changes only weakly, is called “thermal reserve zone”.

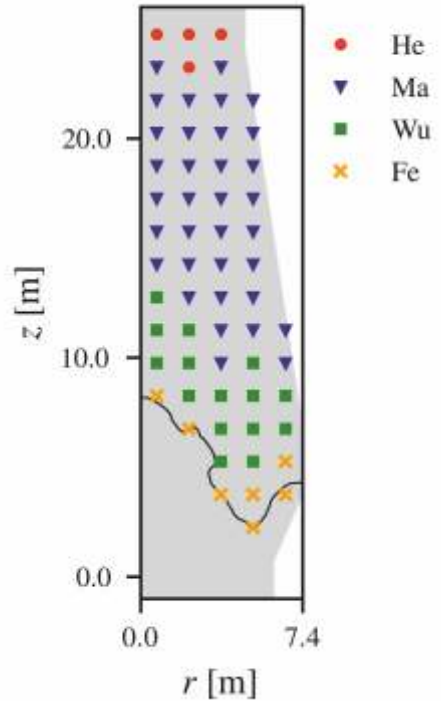


Fig.2: Angle-averaged reduction state. At each point, the prevalent iron oxide is shown. Hematite is rapidly reduced to magnetite. While the next step to wustite takes much longer, the final reduction to iron happens rather quickly again.



EDITORIAL | MACRO

Dear Readers,

Continuum models are mostly an efficient choice for the simulation of macro-scale processes. Especially, using physically-based sub-grid models allows an accurate analysis of industrial-scale gas-solid reactors. However, even the best continuum models fail at certain flow situations. For example, crossing particle jets cannot be appropriately captured by a two-fluid model (TFM), since it lacks of a bi-modal sub-grid velocity distribution (Figure 1). Thus, we proposed a concept for a CFD-DEM magnification lens to connect detailed meso-scale simulations of selected sub-regions with coarse macro-scale TFM analysis, which considerably improves the predictions of the macro-scale model.

Last year we further worked on consolidating our code base, especially the model developed for iron ore reduction (Figure 2). Over the past years, several different implementations have been advanced based on the needs of the different industrial partners and applications. Within the current K1-MET research period, synergies between the different applications and research teams will be used that all partners can benefit from new developments immediately.

Additionally, it has to be outlined that rCFD has successfully been used recently at Borealis to investigate polymerization and process failure at industrial scale.

Finally, I want to thank my team members for their encouragement and their excellent work.



Sincerely,

A handwritten signature in black ink, appearing to read 'Simon Schneiderbauer'.

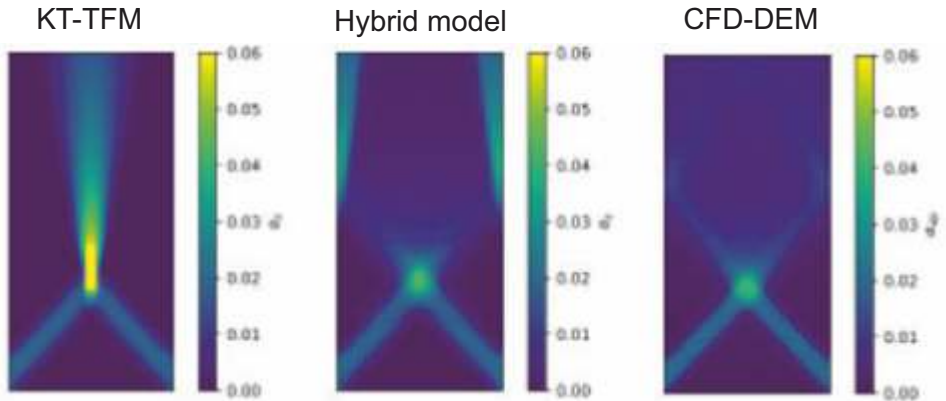
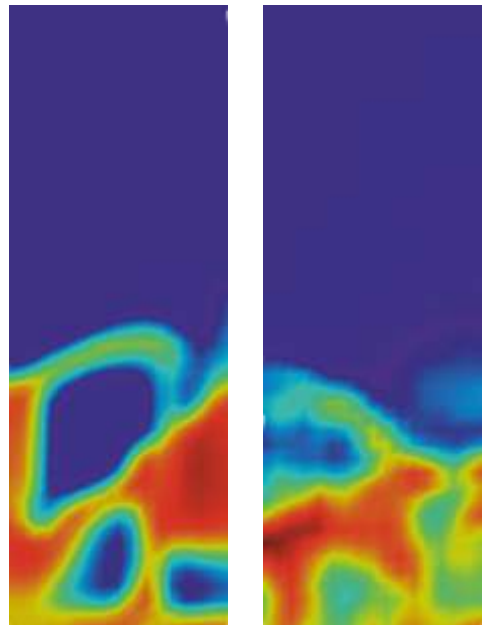


Fig.1: Comparison between the solids volume fraction profiles of KT-TFM, CFD-DEM and hybrid model (CFD-DEM magnification lens) approaches in case of dilute crossing jets problem (jets enter the domain with solids volume fraction of 0.02)

Fig.2: Comparison of a discrete element simulation (DEM, left) and a MPPIC simulation (multi-phase particle in-cell, right) in the case of a bubbling fluidized bed. Since MPPIC does not resolve collision it is more efficient than DEM, but less accurate. However, MPPIC is a key point for the applicability of CFDEMcoupling to large-scale fluidized beds.



MACRO | A HYBRID CONTINUUM-DISCRETE METHOD FOR SIMULATING PARTICLE-LADEN FLOWS

The presence of a dispersed phase (particle phase) gives rise to a broad range of length and time scales that needs to be considered in the modelling of fluid-particle flows. In addition, the large separation of scales observed in particle laden flows, wherein processes happen at the microscale, such as particle collisions and fluid-particle interactions, affect the structures at the macroscale. Therefore, a multiscale modelling strategy which can model fluid-particle flows at different time and length scales with different levels of detail was introduced.

The conventional multiscale modelling strategy is based on the off-line and one-way coupling between the PR-DNS, CFD-DEM and TFM methods. For instance, the PR-DNS is used to derive interphase momentum, heat and mass transfer correlations that can be used in CFD-DEM and TFM approaches. In recent years, the similarities between PR-DNS and CFD-DEM in treating the particle phase and CFD-DEM and TFM in treating the fluid phase and the momentum exchange closures has given rise to hybrid multiscale modelling approaches.

A new hybrid continuum-discrete method for simulating particle-laden flows is developed. This hybrid model applies a CFD-DEM approach within a specific region of interest in a TFM simulation to magnify the continuum particle phase using discrete particles. In the boundaries of the region, the information from the TFM is used to initialize and derive the CFD-DEM simulations while in a region away from the boundaries (two-way coupling region), the CFD-DEM affects the TFM simulation. The back coupling between the CFD-DEM and the TFM simulation is achieved through adding source terms to continuity and momentum equations of the TFM approach in the specific region of interest. This method is capable of changing the unphysical behaviour of the TFM approach to conform to a physical behaviour.

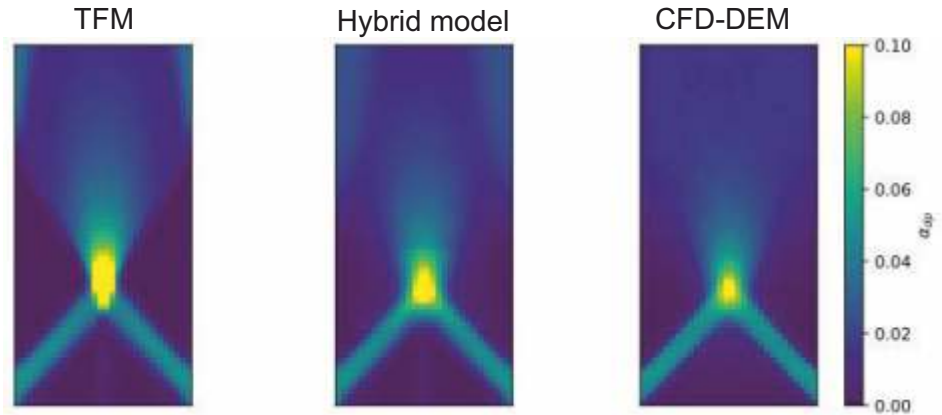


Fig.1: Time averaged solids volume fraction profiles obtained from TFM, CFD-DEM and hybrid model in crossing jet problem (jets enter the domain with solids volume fraction of 0.05).

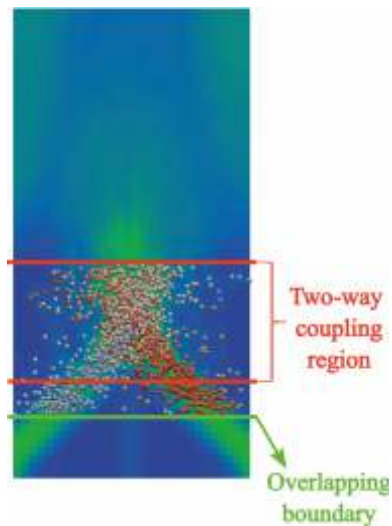


Fig.2: The schematic of the two-way coupling region and overlapping boundary in crossing jet problem. The DEM particles are colored using lateral velocity values.



MACRO | ON THE ROAD TO GREEN STEEL PRODUCTION

Fluidized bed and moving bed reactors are two of the most important technologies in several branches of process industry (steel making, polymer production, carbon capture, fluid catalytic cracking (FCC), biomass reactors). Especially, it is known since decades that fine iron ores can be reduced rapidly and efficiently from iron carrier materials using such devices.

Within the next decades, most of the carbon-based steel production will be transformed to hydrogen-based technologies. Fluidized beds have the potential to become a key technology for this green steel production.

The key advantage in using fluidized beds is that the process step of agglomeration of fine or finest grained iron ores is saved. Nowadays most high quality iron ores are only available in this form (before agglomeration).

Within the metallurgical competence center K1-MET we are exploring together with Primetals Technologies Austria GmbH the numerical analysis of the HYFOR process (hydrogen-based fine-ore reduction) aiming at using finest grained iron ores as raw material.

The figures show results of coarse-grained Euler-Lagrangian simulations, which are founded on physically-based sub-grid models. These simulations yield interesting insights for the development of this technology as well as time-dependent local prediction of the fractional reduction of the ore (Figures 1 and 2). Furthermore, the gas consumption of the process can be estimated.

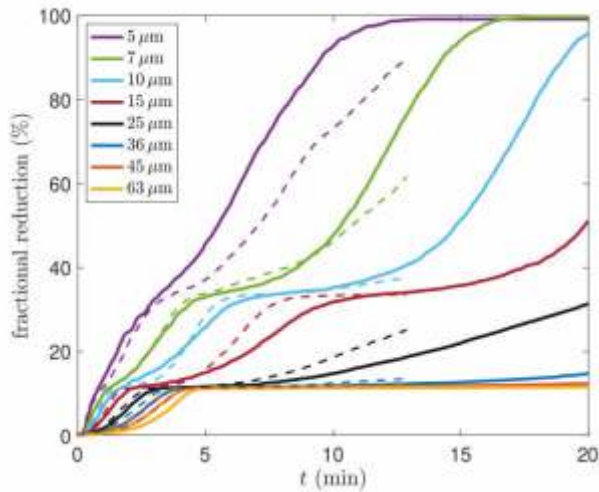


Fig.1: Fractional reduction as a function of the particle diameter for different cohesive materials (solid lines: low cohesion; dashed lines: high cohesion).

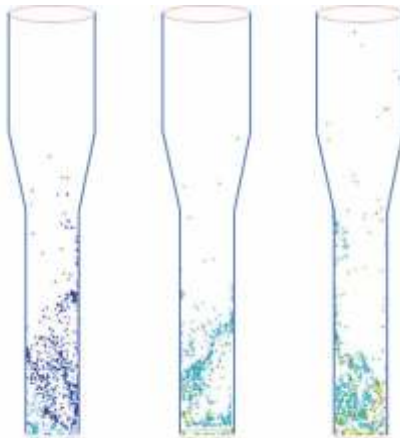


Fig.2: Snapshots of fractional reduction at different times (blue: hematite, cyan: magnetite, green: wustite, red: mostly iron).



MACRO | FAST SIMULATION OF A TUNDISH USING RECURRENCE CFD

The tundish is an important tool used in process industry for many different purposes such as ensuring a smooth flow of metal through the outlet and also the floatation of particle impurities in the metal. As such the flow contains volumes with high and low velocity (Fig.1) and needs both a high resolution and a long simulation time for the simulation in order to properly describe the flow properties.

To do this, instead of running the whole simulation with more costly methods, one can make use of the recurrent properties of the flow and use rCFD to then simulate it for longer time periods. This way, it is possible to do a much shorter simulation with a costly method and then extrapolate the results via rCFD.

As can be seen in Fig.2, the convective behaviour of the flow simulated via DES is properly reproduced using rCFD. On the other hand, the diffusion is not. This can also lead to changed behaviour for residence times in certain parts of the flow (Fig.3) such as sharper peaks. The residence time in the full volume can also deviate if the fluid does not reach the outlet properly because of lack of diffusion.

In order to reproduce the diffusion as well, some calibration schemes also need to be developed in order to further increase the range of applicability for rCFD as well as its ease of use.

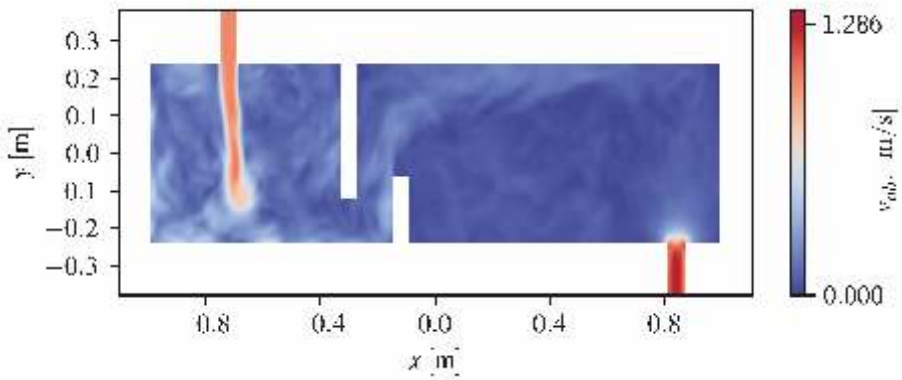


Fig.1: Velocity magnitude on the center plane of a tundish flow simulated via DES.

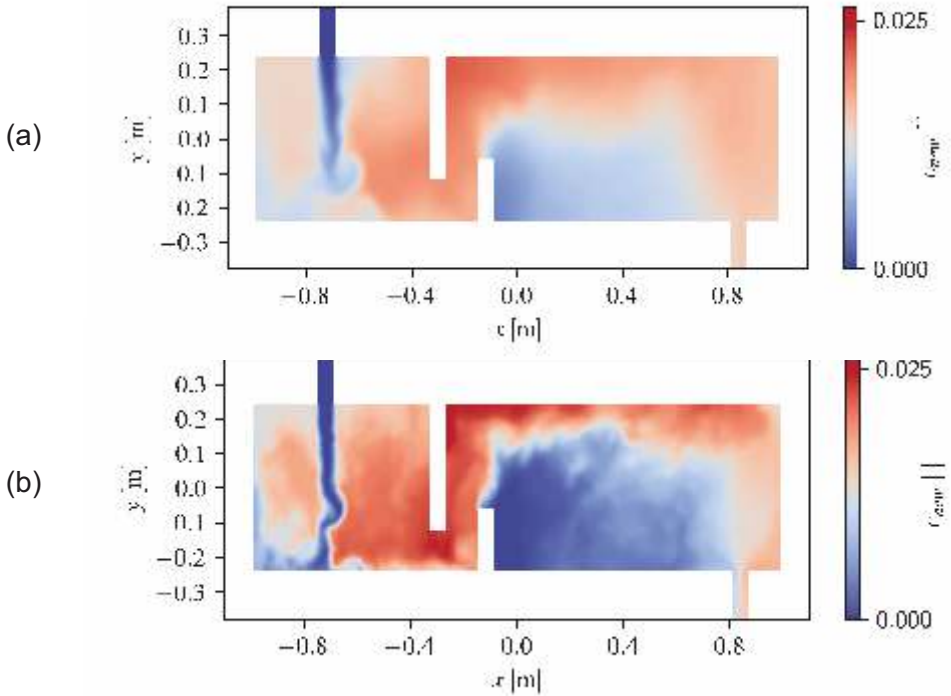


Fig.2: Comparison of a full DES (a) and an rCFD Simulation (b) at a time $t = 26s$. Shown is the concentration of water, which entered the simulated volume through the inlet (top left) between $t = 0s$ and $t = 1s$.

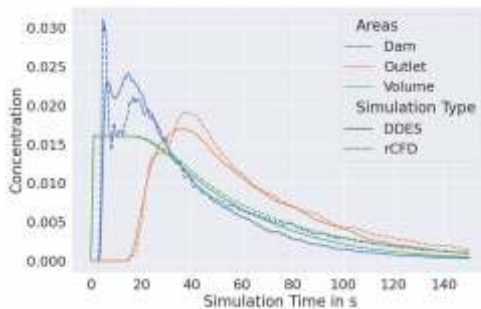


Fig.3: Comparison of residence time between a full DES and an rCFD simulation.



MACRO | DEFLAGRATION

Deflagration describes the very fast and typically uncontrolled as well as undesired combustion of dust particles levitated in gas flows. Consequently, any deflagration event is closely coupled to the characteristics of the fluid-dynamical behaviour of dust particles. Deflagration is particularly important for the safety of different industrial processes including fine dusts.

With joint efforts together with Hoerbiger GmbH and Montanuniversität Leoben, we thoroughly study deflagration events of organic and metallic dusts following a threefold research strategy (i.e. theoretical, numerical and experimental investigations).

Numerically, we employ a Euler-Lagrangian method, where the trajectories of the dust particles are tracked by representative parcels. Since the combustion of dust particles involves relatively high temperatures radiation has to be considered, which is especially important for the particle-particle heat transfer and the ignition using electric sparks.

Comparisons of the predicted flame speed with experimental observations of deflagration events of organic dust in a modified Hartmann tube (Figs. 1 and 2) reveal fairly good agreement. Further efforts have to be put on developing appropriate boundary conditions for radiation and models for the ignition due to electric sparks. Finally, the model should be adapted to metallic dusts, which are of high significance in industrial processes.

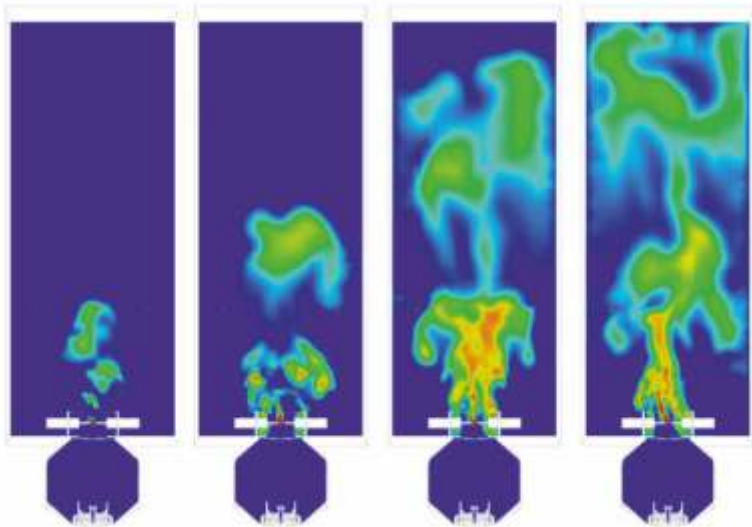


Fig.1: Snap shots of the gas temperature at different times after the ignition by an electric spark (blue: 300 K; red: 2000 K).

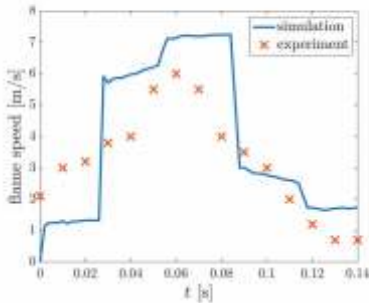


Fig.2: Comparison of numerically predicted flame speed and experimental measurements.

S. Puttinger | S. Schneiderbauer | C. Spijker



EDITORIAL | EXPERIMENTS & DATA ANALYSIS

Dear Readers,

the academic base of our department is fluid mechanics. In the past we therefore tried to isolate the fluid mechanics from other effects in most of our modelling and validation activities. Since multiphase fluid mechanics is challenging enough we tried to keep chemistry out of our lab and felt quite comfortably in our world of inert physics. However, over the last years chemistry was creeping in the back-door and at a certain point we realized that we had slowly given up to ignore the elephant in the room and were already engaged in problems we tried to avoid in the past.

The combustion modelling of dust deflagration was only the starting point of a series of projects that were beyond our previous scope. A focus on Marangoni driven flows has brought us deeply into physical chemistry. And the transition to electricity based steel making is now bringing in plasma physics as a new challenge for modelling and also experimental validation. Once again our annual seminar series proved to be a good kick-starter to get going on unknown ground.



Sincerely,



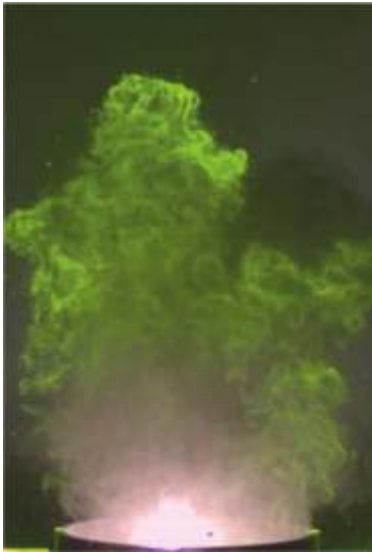


Fig.1: Ignition of a dust cloud of 3g of aluminum powder. The dust cloud has been visualized by a laser light sheet. One can see the initial phase of flame propagation.



Fig.2: The same experiment a few milliseconds later recorded with a second camera running at extremely low exposure time per frame to show the flame structure.

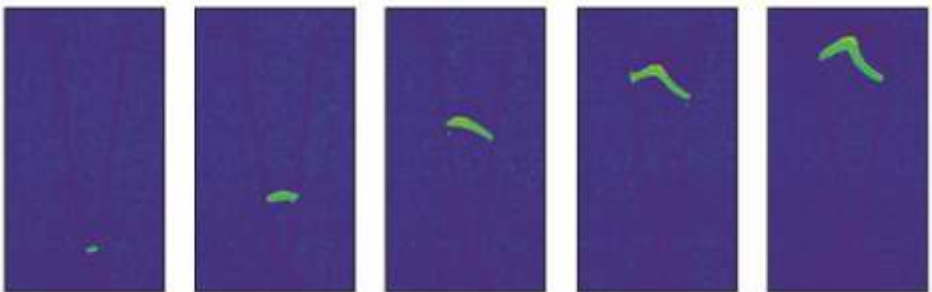


Fig.3: An electric arc is rising in self-induced convection between two diverging electrodes. Images are plotted in false color coding for better visibility.

EXPERIMENTS & DATA ANALYSIS |

DUST DEFLAGRATION

Metallic powders show a very different behavior in dust explosions compared to organic dusts. Organic dust deflagration is dominated by pyrolysis and the subsequent combustion of the volatiles. In contrast, metallic powders like aluminum particles show a reaction behavior that is dominated by radiation. The flame temperature of reacting aluminum particles is much higher and therefore appears extremely bright compared to organic material. Validation experiments with metallic powders are thus more difficult to set up. While for organic powders it is possible to visualize the dust cloud and the flame in a single camera setup (cf. last year's annual report), it is impossible to cover the wide dynamic range of metallic dust explosions with one camera.

Hence, we have modified the test rig that was developed together with colleagues from TPT at Montanuniversität Leoben to have a safe testing environment for metallic powder experiments. The videos are now captured with two separate cameras. The exposure time of camera 1 is set in a way that the dust cloud which is illuminated by a laser sheet is clearly visible (cf. Fig.1 on previous page) and camera 2 is set to extremely low exposure times to capture the flame of the dust deflagration (Fig.1 on the right).

The sequence of post processing is kept the same – we track the vertical expansion velocities of the dust cloud and the flame (Fig.2) as well as their geometrical properties. For aluminum powder the dust cloud shows larger variations than for organic material. We assume that this is mainly caused by the fact that the shape of individual grains is more irregular for metallic dusts than for organic particles. This results in a stronger trend for cluster formation for aluminum powders. Nevertheless, the repeatability of experiments remains very good and the test rig can now be used for a wide variety of materials and dust concentrations.



Fig.1: Image series of a dust deflagration experiment for 5g of aluminum powder recorded at extremely low exposure times. Metallic dusts show a much brighter flame compared to organic dust deflagration (cf. last year's annual report).

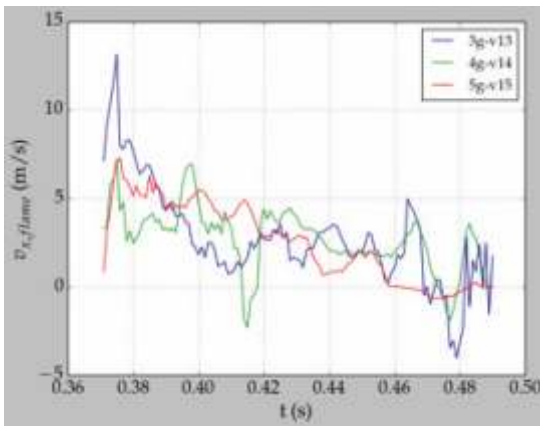


Fig.2: Flame propagation velocities obtained via image processing for cases with 3, 4 and 5g of aluminum powder. Since local particle concentration is high (low volume of the particle cloud before ignition) there is no remarkable difference in the expansion velocity of the flame.

Stefan Puttinger | Christoph Spijker



Stefan Puttinger | stefan.puttinger@jku.at

EXPERIMENTS & DATA ANALYSIS |

DATA COMPRESSION WITH AUTOENCODERS

The idea of recurrence CFD (rCFD) is based on the separation of the involved time scales that can be observed in many flow fields. A lot of systems show a (slow) passive transport of species or temperature on top of (fast) pseudo-periodic behavior. Such recurrent structures of the underlying flow field (e.g. the recurring structures of gas bubbles in a fluidized bed, **Fig.1**) can be described by a recurrence norm and visualized in form of a recurrence matrix. Based on this recurrence matrix the recall of flow snapshots from the underlying database in rCFD is organized.

One of the downsides of rCFD is that such a flow database can easily reach the size of a few gigabytes that need to be loaded into RAM for the rCFD simulation. Even worse, in case of changing boundary conditions several databases need to be loaded. Hence, the used computing hardware imposes certain limits on the scale of the problems that can be solved.

Experiments with autoencoder networks have demonstrated that the size of the original database can be reduced to a few percent of its original extent without losing significant information. Even more it is possible to calculate the recurrence norm and matrix from the so-called latent space in the autoencoder and fully preserve the information that is needed to run an accurate rCFD simulation (**Fig.2**).

But data compression is not the only aspect where neural networks could help to overcome the bottlenecks of rCFD. Generative adversarial networks (GANs) are able to generate artificial snapshots of flow fields that can be used to fill the gaps of limited full CFD databases (**Fig.3**). In addition, networks that are suitable for time series analysis like the long short term memory (LSTM) architecture show the capability to predict plausible flow fields from the history of flow patterns. Hence, in general it would be possible to feed a rCFD simulation with short term predictions from a very limited full resolution database.

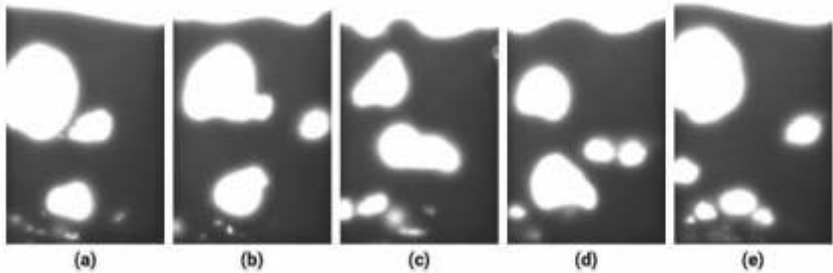


Fig.1: Examples of similar states from experiments in a bubbling fluidized bed test rig. The snapshots are taken at (a) t_0 , (b) $t_0 + 1.06\text{s}$, (c) $t_0 + 5.26\text{s}$, (d) $t_0 + 7.96\text{s}$ and (e) $t_0 + 13.9\text{s}$.

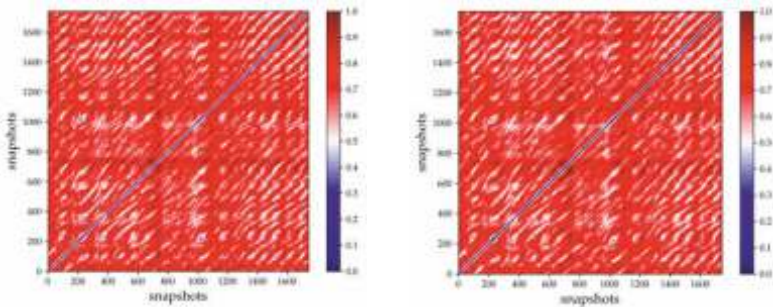


Fig.2: Recurrence matrix of the bubbling bed example based on the original dataset (left) and derived from the latent space representation generated by a convolutional autoencoder (right). The recurrence information is fully conserved in the latent space.

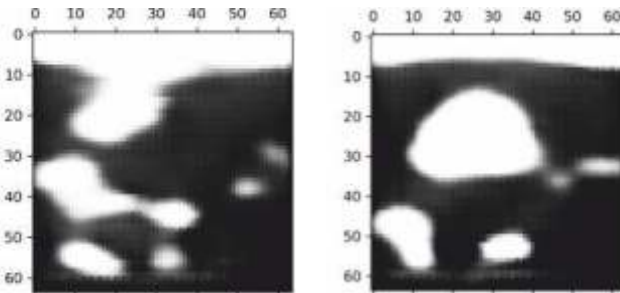


Fig.3: Examples of artificially generated fluidized bed images by a GAN.



EXPERIMENTS & DATA ANALYSIS |

rCFD – VIRTUAL SHADOW DEMONSTRATOR

After the huge success of the rCFD simulation method, the transfer to lab experiments or industrial applications was a logical next step. Together with our partner LCM (Linz Center of Mechatronics GmbH) a user-friendly, interactive exhibition stand is currently under realization, to demonstrate the benefits of the method in virtual shadow or virtual twin configurations.

Finding a well-posed and highly reproducible experimental demonstration setup is quite a challenging task because the rCFD simulation method has certain restrictions. A promising experimental case is the simulation of a temperature field influenced by forced convection. In a first approach the user should establish a thermal stratification, which can be destroyed with a mixer. The goal is to predict the exact temperature state $T(\vec{x}, t)$ of the pseudo periodic flow with rCFD. The real-time capability of rCFD enables the user to instantly validate the prediction of the digital twin by comparing to the actual measurement data.

To guarantee a recurrent flow with adjustable temperature range, a simple bypass system (**Fig. 1**) was created. The simulation setup mimics a cylindrical tank (**Fig. 2**). First results showed reproducible creation and destruction of the thermal stratification (**Fig. 3**).

Further investigations will include full CFD and rCFD simulation to test the applicability of the approach to the setup.

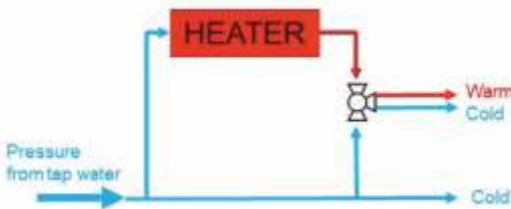


Fig.1: Schematic of the bypass setup. The temperature switch is realized by a three way valve. Warm water is heated by an electric boiler. For continuous flow (equal pressure loss) of both pipes, screw valves are used for regulation.

Fig.2: The cylindrical tank with a stirrer and the inlet flow system. For reducing the inlet momentum, an annular flow supply system on the top and bottom side is used. The outlet nozzle is placed at medium height. Over the tank height several resistance sensors (PT100) are placed to measure the temperature field. The forced convection is achieved by a computer controlled stirrer.

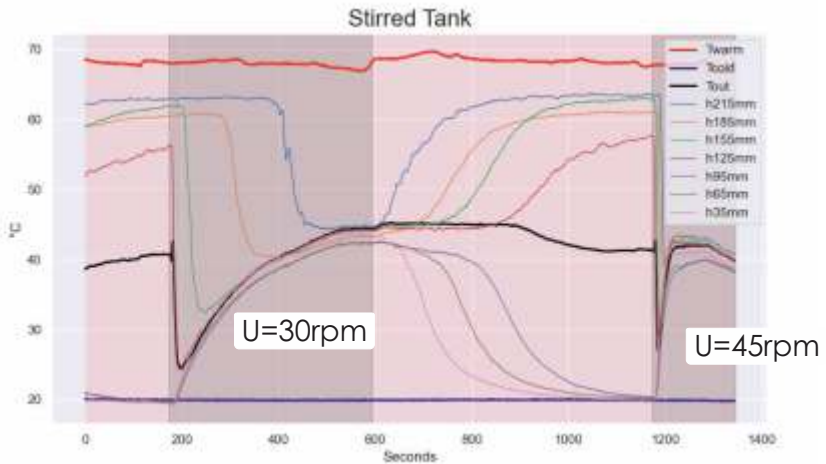
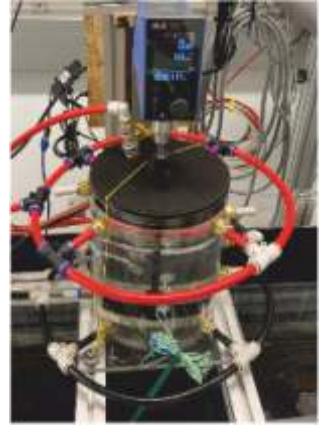


Fig.3: First results as reference data for the rCFD. The time scales for mixing can be influenced by the rotation speed of the stirrer. Thermal stratification is relatively slow and imposes a long repetition time for the experiment. So there is still room for improvement.



EXPERIMENTS & DATA ANALYSIS | BLAST FURNACE TAPPING BEHAVIOR

The recently started project 3.4 in area 3 of K1-MET is focused on hybrid modelling of steel making processes. More specifically, work package 4 is dedicated to the monitoring of blast furnace states and tapping behavior.

Since the blast furnace remains a sort of black box system where mainly input and output parameters are known it is hard to estimate e.g. the current fill level of liquids (liquid steel and slag). However, a good estimate on the liquid levels is crucial for the planning of tapping operations (selection of drill bit, tapping duration, etc.) and to avoid flooding of the tuyeres (which would cause tremendous damage and lead to significant shutdown and repair times).

A major shortcoming to estimate the present state of a blast furnace is the fact that individual signals or measurement subsystems can be faulty or hard to interpret. E.g. thermocouples integrated into the refractory lining can show a large offset or get destroyed over time. Electromagnetic force (EMF) signals have shown capabilities to indicate the fill level inside the furnace but suffer from bad signal to noise ratios (SNR). In addition, recent infrared (IR) recordings of the taphole have shown that pig iron and slag can be distinguished by their radiative properties.

In WP4 we aim to merge the available information from the overall mass balance (production rate), the thermocouple measurements as well as the IR and EMF measurements with a simplified empirical model of the blast furnace drainage behavior. This model will be used for sensitivity analysis of the operating state on various boundary conditions, e.g., we would like to explain the periodic behavior of a sitting and floating dead-man in the hearth of the furnace.

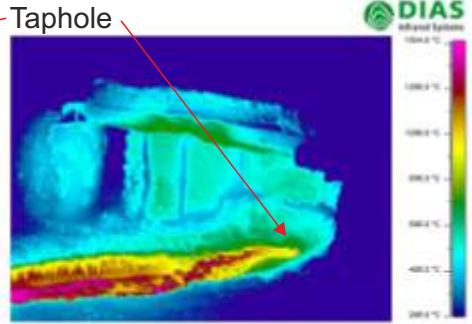


Fig.1: Taphole recorded with a camera in the visual range (left) and the infrared spectrum (right) (images from voestalpine).

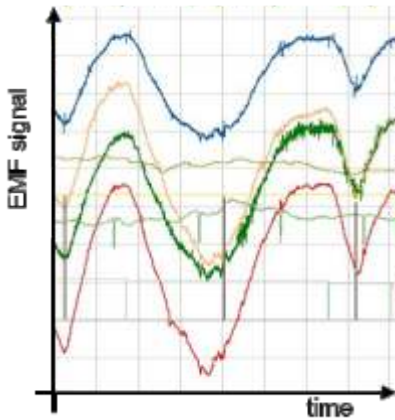


Fig.2: Electromagnetic force signals from blast furnace over two tap cycles (image from voestalpine).

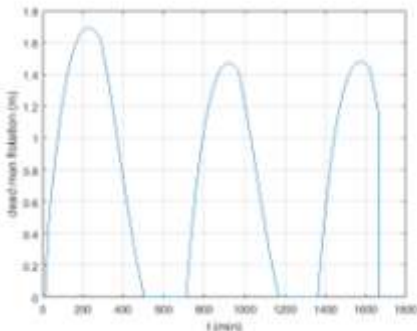


Fig.3: Flotation of deadman based on the simulation model and test data for three tap cycles.



EXPERIMENTS & DATA ANALYSIS | MARANGONI DRIVEN MICRO-DROPLET GENERATION

Further experiments on the production of micro-droplets from water-alcohol mixtures on a substrate liquid of higher viscosity (cf. last year's annual report) have brought a better understanding on the involved effects.

The typical length scale λ at which fingers are formed at the burst diameter decreases exponentially with increasing alcohol concentration. In addition λ is shrinking over time during the evaporation of the core droplet. Hence we can postulate a relation for λ in the form of

$$\frac{\lambda}{r_b} = a_1 + a_2 \phi^{-n} + a_3 \frac{J}{m_0} r_b^2 t$$

with parameters a_1 to a_3 that need to be fitted for different alcohol types and bulk liquids. The fingering wavelength also defines the initial size of the satellite droplets $d_{sd,max}$. Image analysis of the droplets has shown that the size of the satellite droplets decreases linearly on their way outwards (Fig. 2). This leads to two more equations

$$d_{sd,max} = b_1 \ln\left(\frac{\lambda}{r_b}\right) + b_2$$

$$d_{sd}(r) = d_{sd,max} - c_1 \frac{r_{sd}}{r_b}$$

describing the size distribution of droplets for a given system. Recent experiments have demonstrated that this kind of Marangoni effect can also be used to move droplets in lateral channels (Fig. 3).



Fig.3: Droplet moving along a lateral channel in laminar flow. Coalescence of droplets at the flow front forms a characteristic size range that depends on the alcohol concentration.

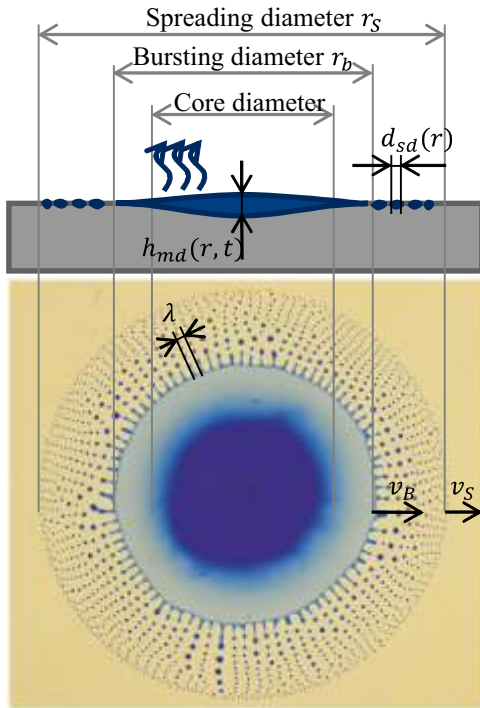


Fig.1: Droplet of water-alcohol mixture (35 wt% isopropyl alcohol) on sunflower oil showing the main geometrical features that are extracted via image processing by warping to polar coordinates.

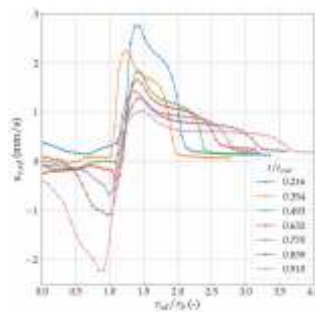
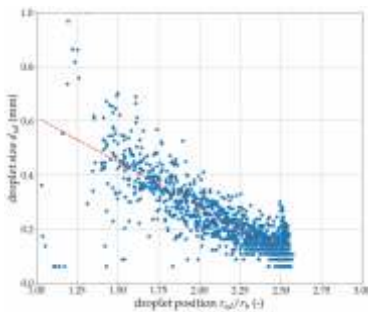
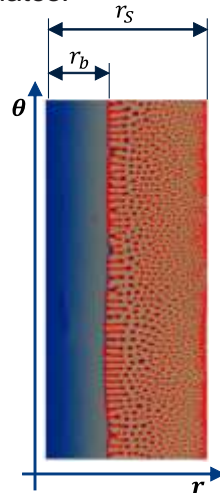


Fig.2: Droplet size distribution over relative radial coordinate (left) and the velocity profiles of outward moving droplets (right).

EXPERIMENTS & DATA ANALYSIS | SELF-SUSTAINED MARANGONI FLOWS

Solvents like ethanol change the surface tension of a bulk liquid. When ethanol evaporates at the surface of the liquid the local concentration gradients drive a fluid motion known as Marangoni flow.

In case of water-ethanol mixtures such concentration gradients are balanced quickly due to the high mobility of the ethanol molecules in the liquid. Adding sodium hydroxide to the water can change the behavior significantly. The presence of NaOH leads to a separation effect, where the local ethanol concentration at the interface is much higher than in the bulk liquid. Concentrated sodium hydroxide solution therefore acts as a good adsorbent, where ethanol can be efficiently stored at the interface, but as a bad absorbent, tolerating only a low concentration of the alcohol in the bulk liquid.

Such an environment for sustained surface tension gradients can drive long lasting motion in the fluid that would entirely be absent in the case of a water-ethanol mixture. For a freely evaporating surface this motion is chaotic. However, by covering parts of the surface with a lid one can further manipulate the ethanol concentration in the gas phase close to the surface and thus imply additional gradients in a certain direction (Fig. 1).

By applying different geometries of the lid cover it is possible to impose specific flow patterns in the liquid (Fig. 2). The flow fields have been recorded via dual-plane PIV in vertical and horizontal direction and show velocities up to several cm/s (the size of the box is 27 x 27 mm).

This work was a joint study with colleagues from JKU and KU Leuven and has recently been published in the high quality journal *Langmuir* that is dedicated to interfacial chemistry.

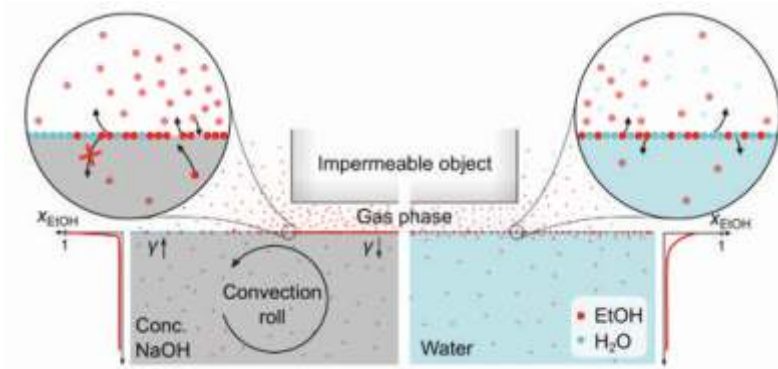


Fig.1: Sodium hydroxide solutions (left) form a thin mono-layer of ethanol molecules while allowing only low concentrations in the bulk liquid. This leads to much higher surface tension gradients compared to water (right).

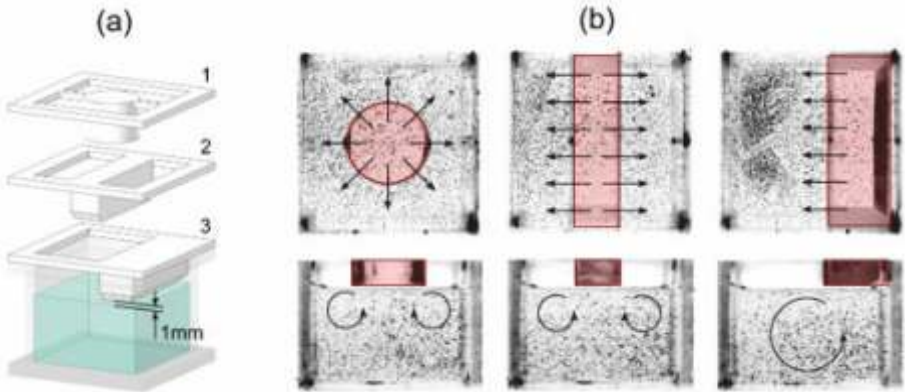


Fig.2: Different lid geometries (a) and the resulting flow patterns (b).



SEMINAR | 15 YEARS OF CURIOSITY ANNUAL PFM SEMINAR

If you want to do science you have to dig deep, persistently pursue your goals and - most important - don't let yourself get distracted!

If you feel aligned with these words, you shouldn't attend our annual seminar. Here, we intentionally distract ourselves from our daily work by jointly looking into something beyond our daily cup of research.

In the past 15 years, we curiously dived into topics as diverse as e.g. granular flow through an hour glass (2010), blood flow (2012, Fig. 1), tsunami wave motion (2013, Fig. 2) or pollutant dispersion (2020, Fig. 3), to name just four of them.

Over the years, different PFM seniors run the seminar by freely following their interests. While Thomas Lichtenegger guided us through Proper Orthogonal Decomposition (2016), Simon Schneiderbauer introduced Turbulence Modelling (2017) and Mahdi Saeedipour shared his enthusiasm on flow physics by his seminars on Micro Fluidics (2018), Marangoni Convection (2021) and Respiratory Flows (2022).

In many seminars, we tried to actually see what we were talking about by creating dedicated experiments of the physical core phenomena. In our actual seminar on Lightning Fluid Dynamics, Stefan Puttinger shot an electric arc hitting onto the surface of a tap water bath in a tuna can. Counter-intuitively for us, we could see surface waves even before the electric arc becomes visible.

On top of our joint internal efforts, we try to invite external experts – as with this year's Claas Bierwisch from the Fraunhofer-Institut in Freiburg.

Yes, our seminars are distracting! But maybe they provide refreshing ideas to problems you have been focusing at for a while...



Fig.1: Seminar 2012 Bloody Fluid Dynamics: This is how we observed our own red blood cells flow through a channel.

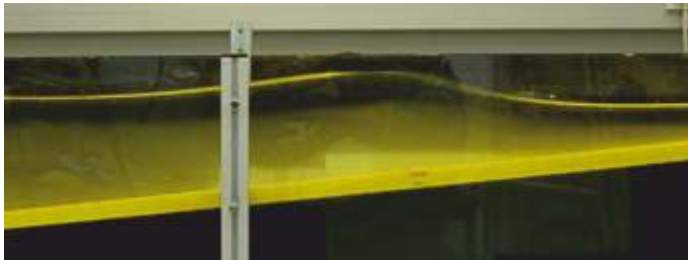


Fig.2: Seminar 2013 Tsunami Models: Wave motion in a water channel.

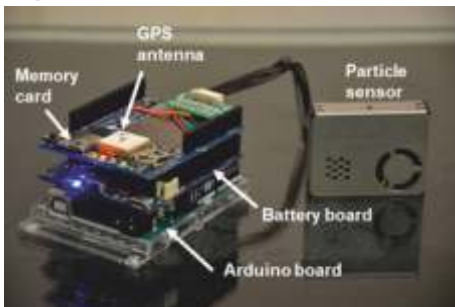


Fig.3: Seminar 2020 Aerosol Measurements: Hand-held Arduino based particle sensor and measurements along a walk through Linz.



SCIENTIFIC FRIENDS | J. Hansson, T. Lichtenegger, S. Pirker, S. Sasic & H. Ström, Chalmers University of Technology & JKU

Particle deposition on submerged objects is of great interest in many industrial applications, such as sensor soiling in the car industry, icing of aircraft and ash build-up in boilers. These build-ups often affect system performance, so a proper understanding of their formation is crucial. Unfortunately, computer simulations of particle deposition are challenging due to the strong separation of time scales between fluid and particles. The rCFD method provides a framework for bridging this gap.

In this work we present an evaluation of the rCFD method as applied to Euler-Lagrange simulations of particle-laden flow around a cylinder (Fig.1). Previous direct numerical simulation (DNS) studies by Haugen and Kragset (2010) have quantified particle-wall impact efficiencies when small spheres are introduced into the flow in front of the cylinder. In this work, we first reproduce the published impact efficiencies in the DNS flow fields by using the less computationally expensive detached eddy simulation (DES) framework. Then, we use a subset of the DES flow field data to generate the rCFD field approximation and generate impact efficiencies in this case as well. Our results (Fig.2) indicate that the impact efficiencies are only to a small degree influenced by the change of flow fields from accurate DNS to an rCFD approximation.

The similar performance in terms of predicted impact efficiency of the traditional CFD and the rCFD approximations indicates that the rCFD method is a viable simulation strategy for Euler-Lagrange-type systems that exhibit strong separation of time scales.

Upcoming research will focus on evaluating the rCFD method for particle deposition studies on more complex geometries. Particular focus will be directed towards snow deposition simulations for cars and car-like geometries.

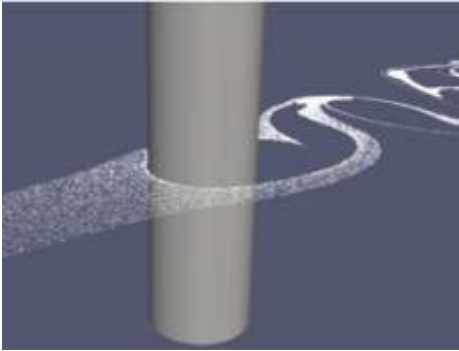


Fig.1: Particle-laden flow around a cylinder. Particles are injected in front of the cylinder and the fraction of particles that collide with the cylinder wall are counted.

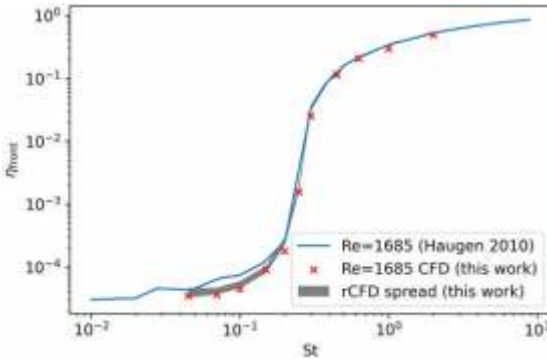


Fig.2: Impact efficiency on the cylinder front surface η_{front} as a function of Stokes number St . The blue line represents DNS reference data, the red crosses are the conventional CFD simulation (DES) results and the gray region is the span of rCFD samples.



johanneh@chalmers.se | thomas.lichtenegger@jku.at | stefan.pirker@jku.at | srdjan@chalmers.se | henrik.strom@chalmers.se

J. Hansson | T. Lichtenegger | S. Pirker | S. Sasic | H. Ström

SELECTED PUBLICATIONS

Esgandari B., Rauchenzauner S., Goniva C., Kieckhefen P., Schneiderbauer S.: A comprehensive comparison of Two-Fluid Model, Discrete Element Method and experiments for the simulation of single- and multiple-spout fluidized beds, in *Chemical Engineering Science*, Vol. 267, 118357, 2023

Doppelhammer N., Puttinger S., Pellens N., Voglhuber-Brunnmaier T., Asselman K., Jakoby B., Kirschhock C., Reichel E.: Generation and Observation of Long-Lasting and Self-Sustaining Marangoni Flow, in *Langmuir*, ACS Publications, 2023

Kronlachner T., Pirker S., Lichtenegger T.: Block-movement-based calibration of a discrete element model for fine, cohesive powders, in *Powder Technology*, Vol. 421, 2023

Porcaro C., Saeedipour M.: Hemolysis prediction in bio-microfluidic applications using resolved CFD-DEM simulations, in *Computer Methods and Programs in Biomedicine*, Vol. 231, Seite(n) 107400, 2023

Puttinger S., Spijker C., Schneiderbauer S., Pirker S., Meyer G., Buchner C., Kerbl A.: Dust Cloud Evolution and Flame Propagation of Organic Dust Deflagration under Low Wall Influence, in *Journal of Loss Prevention in the Process Industries*, Vol. 83, Nr. 105042, 2023

Saeedipour M.: An enstrophy-based analysis of the turbulence-interface interactions across the scales, in *International Journal of Multiphase Flow*, Vol. 164, Seite(n) 104449, 2023

Zhang X., Pirker S., Saeedipour M.: Numerical investigation of particle motion at the steel-slag interface in continuous casting using VOF method and dynamic overset grids, in *Experimental and Computational Multiphase Flow*, Vol. 5, Springer, Seite(n) 178–191, 2023

Imprint:

DEPARTMENT OF PARTICULATE FLOW MODELLING

T +43 (0)732/2468 6477 | **F** +43 (0)732/2468 6462 | **W** <http://www.particulate-flow.at>

P | Altenbergerstrasse 69 | 4040 Linz | Austria

